Journal of Physics: Conference Series **160** (2009) 012019 doi:10.1088/1742-6596/160/1/012019

Detection of K^+ Mesons in Segmented Electromagnetic Calorimeters

D.I. Glazier, T.C. Jude for the CrystalBall@MAMI and A2 collaborations.

School of Physics, University of Edinburgh, Kings' Buildings, Edinburgh, EH9 3JZ, UK

E-mail: dglazier@ph.ed.ac.uk

Abstract. The combination of the CrystalBall and TAPS electromagnetic calorimeters were installed in the MAMI A2 hall in 2003. Here they are able to detect the reaction products from photo-induced reactions in combination with the Glasgow photon tagger. In the last two years the MAMI facility was upgraded from 885 MeV to 1.5 GeV, the A2 photon tagger underwent a similar upgrade crossing the threshold for strangeness photoproduction. For the CrystalBall this created a new challenge, to identify K^+ mesons above the large background from other charged hadrons, in a situation where the detector setup does not benefit from a magnetic field to help separate particle species. These proceedings outline a novel technique which uses the decay products of the K^+ as a strangeness tag.

1. The CrystalBall at MAMI

Since 2003 the CrystalBall and TAPS electromagnetic calorimeters have been the central detectors facilitating experiments in the tagged photon hall (A2) at the MAMI electron accelerator facility. The close to complete acceptance for photons make it an ideal site for investigations of the photoproduction of neutral mesons. In addition, complimentary detector systems have successfully extended the range of particles that can be analysed in the calorimeters allowing a more diverse range of photoproduction experiments to be performed.

1.1. MAMI

The Mainzer Microtron (MAMI) [1, 2], is a well established electron accelerator providing an extremely high quality electron beam. An energy upgrade was completed in 2007 increasing the beam energy from 885 MeV (MAMI-B) to 1.5 GeV (MAMI-C). Crucially this crossed the threshold for associated strangeness production where kaons are produced in tandem with a hyperon (Λ or Σ).

1.2. The Tagged Photon Hall (A2)

In the A2 tagged photon hall the MAMI e^- beam is converted into a real photon beam via bremsstrahlung. The residual e^- from this process are momentumanalysed in a magnetic spectrometer, developed by the University of Glasgow. This tagger can be used to analyse up to $10^8\gamma s^{-1}$ and photon energies between 5-92 % of the incident electron beam energy. The 352 scintillators in the focal plane provide a photon energy resolution of around 2 MeV with a 1.5 GeV beam. An additional "microscope" can be installed to improve the resolution to

sub MeV for precision experiments. The photon beam can be circularly polarised up to 80 % through transfer from longitudinally polarised electrons, or, linearly polarised through coherent bremsstrahlung in an aligned diamond radiator also up to 80 %. In parallel with the MAMI-C upgrade the tagger underwent a successful upgrade of its own [3]. The magnetic field was increased to allow the bending of 1.5 GeV electrons while the focal plane detectors were replaced and electronics revamped.

The A2 collaboration have available a number of target systems including cryogenic Hydrogen, Deuterium and ^{3}He, a wide range of solid nuclear targets such as Carbon, Calcium and Lead and will soon have a number of polarised targets for experiments on Hydrogen, Deuterium and ^{3}He.

1.3. CrystalBall

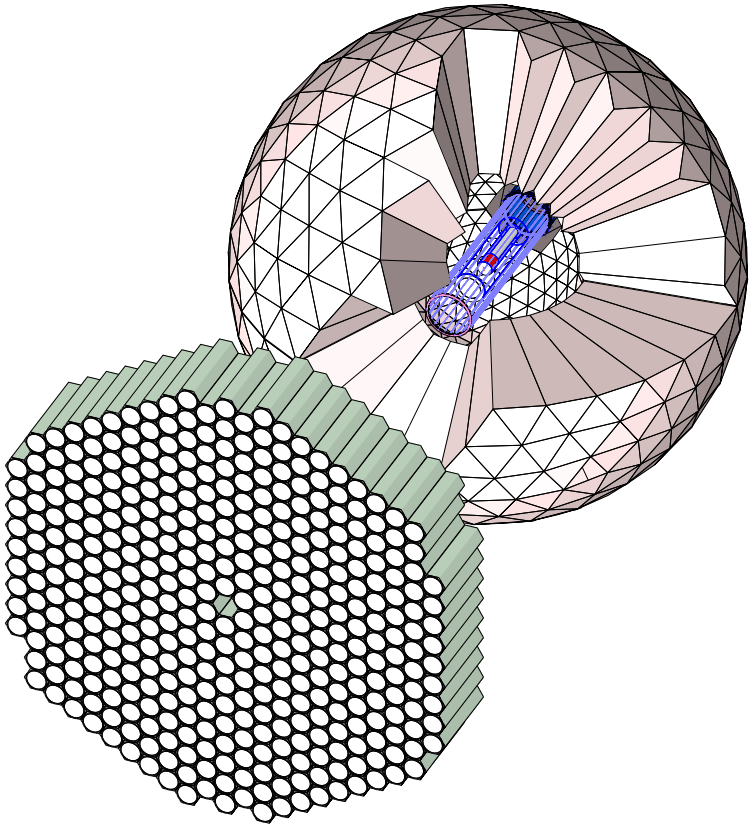

Figure 1. The CrystalBall and TAPS calorimeters as arranged in the A2 hall. Shown inside the ball are the PID detector and Hydrogen target.

The CrystalBall is a well traveled calorimeter [4]. Conceived and built at SLAC in the 1970s it has been the central detector system for experiments at SPEARS, DORIS and BNL prior to arriving at MAMI. It consists of a segmented array of 672 NaI crystals spherically arranged around the target. Each crystal is a 41 cm long truncated pyramid which is equivalent to 15.7 radiation lengths. This arrangement covers 93 % of phase space leaving two holes at the front and back for the incident beam to pass through. Photons traversing into the crystals will produce an electromagnetic shower contained typically in less than 13 neighbouring crystals, analysis of which provides the energy and direction of the initial photon. The granularity provides angular resolution of approximately 2° and the NaI crystals light output characteristics enable an energy

resolution of $\sigma_E = 2.0\%E^{0.36}$. By considering multiphoton final states neutral mesons such as the π^0 and the η can be identified and their 4-momentum reconstructed.

Each crystal is fitted with a photomultiplier the output of which is split 3 ways, the first to the event trigger, the second to a multi-hit TDC and the third to a 40 MHz sampling ADC. As well as sampling the main signal the ADCs are recorded before and after and event trigger to allow subtraction of remnant light [5, 6]. The timing resolution consists of a 3 ns component from the trigger timing and a 2 ns component intrinsic to each crystal. For the technique outlined in this paper it is the relative time resolution of 2 ns which is of importance.

1.4. TAPS

For fixed target experiments such as those performed in the A2 hall the forward angular region is particularly important. The CrystalBall has a hole in this region covering approximately 0-20°, so to increase the acceptance in this crucial region of phase space the TAPS electromagnetic calorimeter has been installed. The TAPS detector has featured prominently in previous A2 experiments as well as spending time at ELSA, GSI, Ganil and CERN. Since the upgrade to MAMI-C, TAPS has been positioned 1.45 m upstream from the target and consists of 384 BaF_2 crystals. Each crystal is hexagonally shaped and 25 cm, or 15 radiation lengths long. The energy resolution $\sigma_E = 2.5\%E$ while the angular resolution is around 1°. The fast component of the BaF_2 crystals coupled to constant fraction discriminators facilitate a timing reolution of 1 ns.

1.5. Additional Detector Systems

As mentioned previously the CB and TAPS calorimeters are excellent γ detectors. However to increase their potential two additional detector systems have been added. Firstly 2 cylindrical MWPCs have been installed inside the CB. These provide accurate track information ($\sigma_\theta \simeq 1°$) as well as a vertex position.

Secondly a particle ID detector (PID) [8] is installed inside the wire chambers. This consists of 24x50cm long plastic scintillators orientated parallel to the beam direction. The scintillator thickness is 4 mm and it thus provides a ΔE signal which allows a separation of charged pions, protons and deuterons.

2. Outline of Physics Programme

Such a versatile detector system covering almost all accessible phase space coupled to an intense high resolution photon beam allows for an ambitious and diverse programme of experiments. The main themes of the MAMI programme include, precision determination of nucleon resonance properties, tests of fundamental symmetries and test of low energy theorems. A few experiments from the programme are described below.

The provision of polarised beam and targets provides an excellent basis for measurements of meson photoproduction. In addition the development of large acceptance recoil nucleon polarimetry will allow for the first time sufficient observables for 'model independent' measurement of the photoproduction amplitudes. This will aid our understanding of the nucleon excitation spectra as well as the underlying reaction mechanism.

The upgrade to 1.5 GeV beam energy also makes MAMI-C a competitive η factory. The large acceptance for photon detection allows precision measurements of the subsequent decay, in particular rare decays, providing stringent tests of fundamental symmetries. In addition decay to $3\pi^0$s provides sensitivity to the $\pi\pi$ scattering length.

The multiparticle final state detection, coupled with the high luminosity photon tagger, enables measurements where a very accurate and comprehensive determination is required to extract the important physics, for example radiative resonance decay. In particular, measurement of the $N\pi\gamma$ final state with polarised beam is sensitive to the magnetic moment of the $\Delta^+(1232)$, providing a route to measure this poorly known quantity.

There is also many physics opportunities that will be investigated with nuclear targets such as medium modifications of the ω meson and multinucleon knockout experiments. The first publication from the collaboration used a nuclear target and the ability of the CB to measure nuclear decay γs to investigate incoherent π^0 production on Carbon [8], which allows access to transition matter form factors and the $N\Delta$ interaction. A similar measurement of coherent π^0 production on Lead will allow an extraction of the neutron skin thickness which is a crucial quantity for nuclear physics and the physics of neutron stars.

3. K^+ Photoproduction

K^+ photoproduction is an important tool in baryon spectroscopy as it is naturally sensitive to resonances with strong strangeness decay branches. This may included a number of missing resonances predicted by the quark and other phenomenological models but as yet unseen in partial wave analysis of pion scattering data. A number of experiments have already been completed at ELSA, CLAS and GRAAL although some cross section results are inconsistent [9]. Another aspect of K^+ production that is particularly suited to study at the upgraded MAMI-C is threshold production. In this regime accurate data will provide a test of Low Energy theorems such as Chiral Perturbation Theory.

4. K^+ Detection

One of the crucial requirements of any detector system is being able to distinguish between different particle species. Commonly this is done through measurement of two variables from momentum, energy or velocity therefore determining the mass of the particle. For the CB the short distance between the target and crystals as well as the considerable length of the crystal preclude a sufficiently accurate extraction of velocity from time of flight. In practise the CB can only directly determine the kinetic energy of the particle through calorimetry and a combination of the CB and PID detector energy signals allows separation of protons and pions using the standard ΔE-E analysis.

This method however is not sufficient for separating K^+ due to a number of factors. Firstly detector resolution and hadronic interactions in the CB crystals make it impossible to separate the kaons from the several orders of magnitude greater incidence of protons in the CB. Secondly the K^+ will likely decay within the ADC sampling time making the energy deposited in the ball invalid for ΔE-E analysis. However this second factor can instead be used to our advantage to actually tag the presence of the K^+ as outlined in the following two sections.

4.1. K^+ Decays

The K^+ undergoes a Weak decay with a lifetime of 12 ns, significantly larger than the CB resolution of 2 ns, but well within the standard TDC sampling time used of 200 ns. For the majority of cases the K^+ will stop in the CB crystals after around 1ns and then decay at rest some time later. The two main decay channels are,

- $K^+ \rightarrow \mu^+\nu_\mu$ 63.51% (muonic)
- $K^+ \rightarrow \pi^0\pi^+$ 21.16% (pionic)

In the case of the muonic decay the neutrino will leave undetected while the muon will deposit the 152 MeV kinetic energy from the decay kinematics. This energy allows the muon to travel 25 cm through the CB and pass through around 5 crystals. The muon itself will also decay but its lifetime of 2 ms means its decay will generally not register in the CB TDCs. In the pionic decay all of the kinetic energy and mass of the π^0 can be contained inside the CB, whereas the π^+ will deposit just its kinetic energy of 109 MeV plus 3 MeV from its own muonic decay. This results in up to 360 MeV ($M_K - M_\pi$) being deposited in a large number of crystals around the original K^+ hit crystal.

4.2. K^+ Tagging Algorithm

The procedure developed for identifying a K^+ through its decay is as follows,

(i) Construct as large a cluster of crystal hits as possible through combining neighbouring hits.

(ii) Split this cluster into separate side clusters according to the timing of the hits. i.e. each side cluster contains hits with timing signals within 8 ns of each other.

(iii) The main cluster that occurs first in time is identified as the incident K^+, while the second side cluster is due to its decay.

(iv) Cut on the second side cluster energy ($> 100MeV$),average time of hits relative to the K^+ ($> 10ns$), length from the K^+ cluster to furthest crystal in decay cluster ($> 11cm$) and number of crystals (> 1) to select the K^+ muonic and pionic decay candidates.

(v) If the second side cluster passes the cuts check the first cluster passes a ΔE-E analysis.

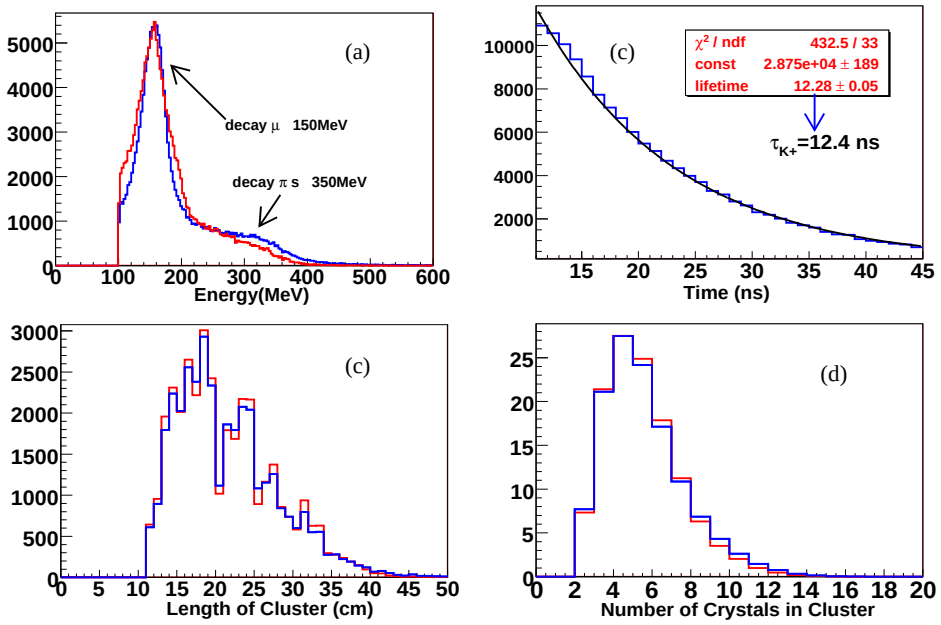

Figure 2. The plots show the energy, time, length and number of crystals in the second clusters. The second cluster cuts and ΔE-E analysis have been applied. The blue line shows the plots from real data samples, whereas the red line shows the result from a GEANT4 simulation of K^+ photoproduction events. The 150 MeV μ^+ peak is clearly seen in the energy spectra while the time spectra (real data only) shows the K^+ lifetime.

5. Data Analysis

This technique was developed using both real experimental data and a detailed GEANT4 [10] simulation of the A2 CB detector systems [11] using K^+ photoproduction events. The simulation shows the technique works well for both the CB and TAPS calorimeters, however as data has only been collected under trigger conditions that allow K^+ to be detected with the CB the following analysis will concentrate on only that detector. The plots in figure 2 show the comparison of the experimental data and simulation for the characteristics of the second side cluster after the algorithm of the previous section has been applied. The simulation gives a very good overall description of the data. The differences in the energy spectra, fig. 2a are attributable to acceptance effects arising because of the difference in angular distribution of K^+ in the phase

space simulation compared to the data. The μ^+ energy of 150 MeV is particularly prominent in the energy spectra, with the pionic decay events forming the higher energy shoulder. The timing spectra, fig. 2b, show an exponential decay consistent with the K^+ lifetime, this is the same for the simulated data. The distribution of decay cluster length, fig. 2c, and multiplicity, fig. 2d, also show very good agreement with the simulation.

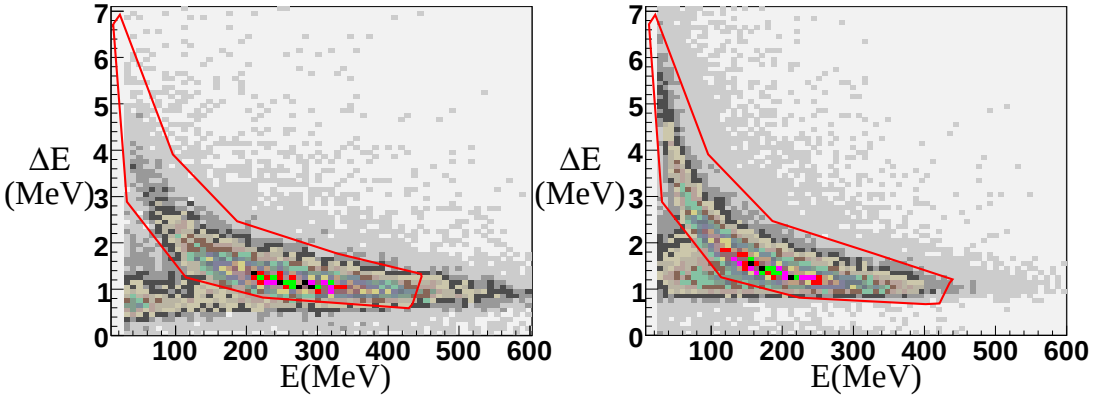

Figure 3. The real (left) and simulated (right) ΔE-E analysis. The red region shows the events selected as K^+

The additional constraint on the ΔE-E analysis is shown in figure 3 where the K^+ cluster energy is plotted versus the PID signal. A ridge consistent with that expected for K^+ is clearly visible. The red cut region is effective for suppressing any residual π^+ background. With all cuts applied the K^+ detection efficiency is around 10 % for K^+ up to 330 MeV.

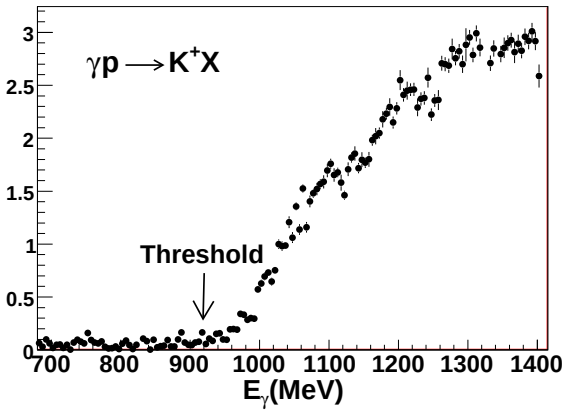

Figure 4. The raw K^+ excitation spectra taken from real experiment showing the reaction threshold of 920 MeV.

6. Some Preliminary Photoproduction Results

Already some data has been taken with the 1.5 GeV circularly polarised beam and the hydrogen target. Presented here are the very preliminary first results from analysis of this data with the new technique. Figure 4 shows the K^+ yield as a function of photon beam energy, uncorrected for acceptances. The main point to observe here is the spectrum shoots up at the $K^+\Lambda$ threshold of around 920 MeV photon energy, with little background below this supporting the validity of the technique for selecting the kaons. In addition, the missing mass of the beam, target and K^+ system has been reconstructed in fig.5. The two most probable reactions in our energy range

are $K^+\Lambda$ and $K^+\Sigma^0$ production and the masses of these two particles are clearly seen in the missing mass spectra. The left panel shows the real data with peak width and position consistent with the simulation on the right, note that an equal number of Λ and Σ^0 were assumed in the simulation. The separation is already at a reasonable level, but the missing mass resolution will be improved further when the wire chambers are fully implemented giving more accurate track information for the K^+. An energy loss correction, not yet implemented, will further increase the separation. The two channels may also be separated through the radiative decay of the Σ^0 to a Λ by detecting the decay photon with energy of the order of 100 MeV, in coincidence in either the CB or TAPS.

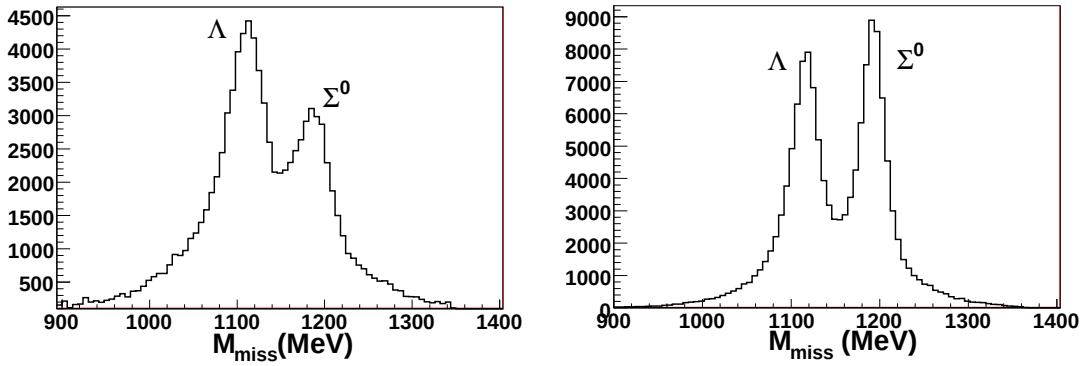

Figure 5. The missing mass of the beam+target-K^+ system, showing the masses of the Λ and Σ^0 associated with the K^+ production. The left hand panel is real data, the right simulation assuming an equal number of Λ and Σ^0 events.

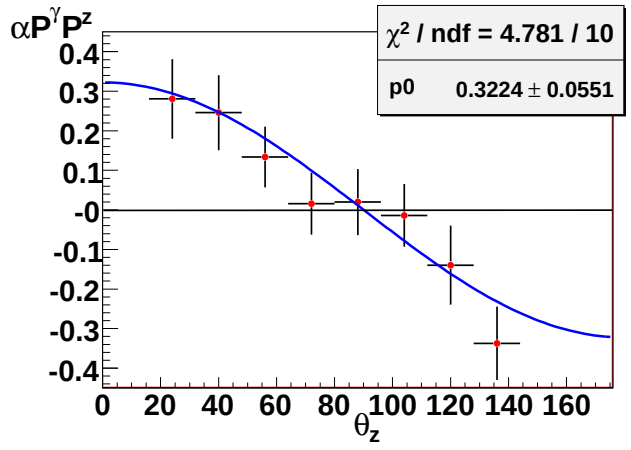

Figure 6. The asymmetry of the decay neutron with respect to the Λ momentum direction and beam helicity.

The angular distribution of the Λ weak decay is sensitive to its polarisation. With our detector we are able to detect either the decay to $\pi^0 n$ (36%) or $\pi^- p$ (64%). In these decays the polarisation P^i, with respect to a given axis i, is related to the angular distribution of the nucleon with respect to that axis via,

$$N(\theta_i) = N_0\left(1 + \alpha P^i \cos\theta_i\right)$$

where $\alpha = 0.64$ is the Λ asymmetry parameter. Flipping the direction of the polarisation via the beam helicity allows us to form an asymmetry out of this distribution, we can thus

deduce the polarisation transferred from the incident circularly polarised photon beam, P^{γ}, to the recoiling Λ,

$$A\left(\theta_i\right) = \frac{N^{+} - N^{-}}{N^{+} + N^{-}} = \alpha P^{\gamma} P^{z} \cos\theta_i$$

Figure 6 shows this asymmetry for an axis defined along the Λ momentum direction and the decay to $\pi^0 n$. This preliminary analysis already shows a clear asymmetry related to the polarisation transfer.

References

[1] H. Herminghaus, K.H. Kaiser, H. Euteneuer 1976 *Nucl. Instrum. Methods.* A **138** 1
[2] T. Walcher 1990 *Prog. Part. Nucl. Phys.* **24** 189
[3] J.C. McGeorge *et al.* 2008 *Upgrade of the Glasgow photon tagging spectrometer for Mainz MAMI-C Eur. Phys. J.* A i2007-10606-0
[4] A. Starostin *et al.* 2001 *Phys. Rev.* C **64** 055205
[5] D. Krambrich, Ph.D. thesis, Universitat Mainz, 2006
[6] D.P. Watts 2004 *Calorimetry in Particle Physics: Proceddings of the 11th Int. Conf., Perugia, Italy* (Singapore, World Scientific) edited by C. Cecchi *et al.* p560
[7] R. Novotny 1991 *IEEE Trans. Nucl. Science* **38** 379
[8] C.M. Tarbert *et al.* 2008 *Phys. Rev. Letts.* **100** 132301
[9] J.W.C. McNabb *et al.* 2004 *Phys. Rev.* C **69** 042201
[10] S. Agostinelli *et al.* 2003 *Nucl. Inst. Meths.* A **506** 250-303
[11] http::/www.ph.ed.ac.uk/nuclear/G4